

# Length scale for the onset of Fickian diffusion in supercooled liquids

LUDOVIC BERTHIER<sup>1,2</sup>, DAVID CHANDLER<sup>3</sup> and JUAN P. GARRAHAN<sup>4</sup>

<sup>1</sup> *LDV UMR 5587, Université Montpellier II and CNRS, 34095 Montpellier, France*

<sup>2</sup> *Rudolf Peierls Centre for Theoretical Physics, University of Oxford, 1 Keble Road, Oxford, OX1 3NP, UK*

<sup>3</sup> *Department of Chemistry, University of California, Berkeley, CA 94720-1460, USA*

<sup>4</sup> *School of Physics and Astronomy, Univ. of Nottingham, Nottingham, NG7 2RD, UK*

PACS. 05.20.Jj – Statistical mechanics of classical fluids.

PACS. 05.70.Jk – Dynamic critical phenomena.

PACS. 64.70.Pf – Glass transitions.

**Abstract.** – The interplay between self-diffusion and excitation lines in space-time was recently studied in kinetically constrained models to explain the breakdown of the Stokes-Einstein law in supercooled liquids. Here, we further examine this interplay and its manifestation in incoherent scattering functions. In particular, we establish a dynamic length scale below which Fickian diffusion breaks down, as is observed in experiments and simulations. We describe the temperature dependence of this length scale in liquids of various fragilities, and provide analytical estimates for the van Hove and self-intermediate scattering functions.

*A ten-day journey starts with a single step. — Lao-tse, Tao Te King.*

In this paper, we consider the process of self-diffusion of probe molecules in supercooled liquids. Figure 1 shows the trajectory of a such a probe obtained from a model of a supercooled liquid [1]. At conditions shown, the structural relaxation time of the model is of the order of  $10^5$  microscopic time steps. The left panel of Fig. 1 extends over this range of time. The right panel extends three orders of magnitude longer in time, and one order of magnitude larger in space. Here, the trajectory looks like a random walk of Fickian diffusion, unlike the trajectory in the left panel. In this paper, we describe the crossover from non-Fickian to Fickian diffusion, and identify the length scale,  $\ell^*$ , that characterizes the crossover.

In our perspective supercooled liquids are modeled by a coarse-grained mobility field evolving with simple empirical rules [2]. An essential prediction of our modeling is that dynamics becomes spatially correlated [3], i.e., the growth of timescales is accompanied by the growth of dynamical lengthscales, giving rise to the phenomenon of dynamic heterogeneity observed in experiments and simulations [4–7]. This finding suggests a degree of universality and thus utility for a coarse-grained perspective. Nevertheless, it is important to test of our approach by using it to revisit all sorts of experimental and numerical studies of supercooled liquids [1,8–10]. Generic properties are only weakly dependent upon details of the models, which become important, however, for quantitative comparisons to experiments or simulations [8]. In most of this paper we will therefore pursue our investigations in the simplest lattice model of this family [2], namely the one-dimensional Fredrickson-Andersen model (hereafter 1D FA model) [11].

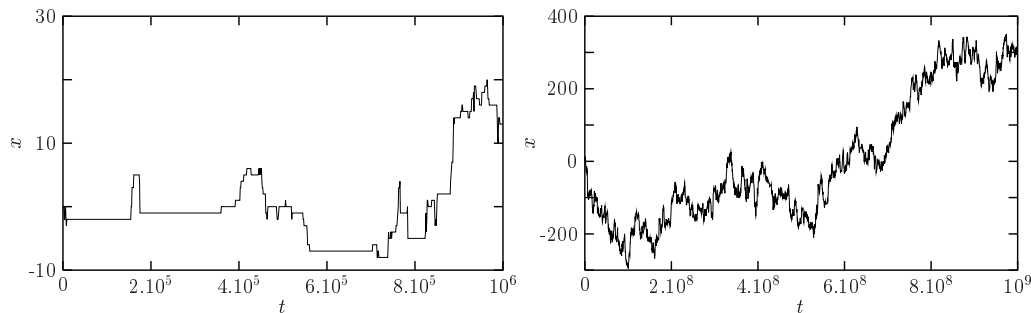


Fig. 1 – A typical trajectory of a probe molecule in the 1D FA model at  $T = 0.25$  is shown twice on different time and length scales. The  $\alpha$ -relaxation time is  $\tau_\alpha \sim 10^5$ , the diffusion constant  $D \sim 10^{-4}$ .

This is defined by the Hamiltonian  $H = \sum_i n_i$ , where  $n_i = 0, 1$ , with dynamics constrained by isotropic dynamic facilitation. A site needs at least one neighbour with  $n_i = 1$  to change state, with Boltzmann probability. The concentration of excited sites is  $c = \langle n_i \rangle = [1 + e^{1/T}]^{-1}$ ,  $T$  being the temperature. Lengths are in units of the lattice spacing which we set to one.

Self-diffusion is studied by introducing a probe molecule [1], which makes it possible to map ‘spins’ back to ‘particles’. The probe’s position,  $x(t)$ , evolves with reduced time as  $x(t+1) = x(t) \pm n_x(t)n_{x\pm 1}(t)$ , i.e., the probe is allowed to move only when sitting on an excitation and jumps to a neighbouring excited site. Due to coarse-graining, fast vibrations are ignored. In that sense, our results are close to dynamic studies of inherent structures [13,14], but this is not crucial as far as the long-time relaxation is concerned. Numerically, we studied the dynamics of probe molecules in the 1D FA model using Monte Carlo simulations. At each temperature, the system size,  $L$ , is chosen to be much larger than the mean distance between excitations,  $\ell(T) = 1/c(T)$ , in order to avoid finite size effects. We typically used  $L > 10\ell(T)$  and averaged over at least  $10^4$  independent probe trajectories. We have also studied the behavior of a probe in the East model [12], a more constrained and fragile counterpart of the 1D FA model, and results are briefly discussed near the end of the paper.

The trajectories in Fig. 1 show the typical time evolution of the position of a probe molecule in the 1D FA model at a fixed, low temperature. Due to the kinetic constraint, excitations in dynamically facilitated models propagate as continuous excitation lines in space and time [1,3]. On the  $\alpha$ -relaxation timescale motion is non-Fickian with long periods where the molecule is immobile, seen as plateaux in Fig. 1, punctuated by shorter periods where it travels over a few sites. Plateaux correspond to the particle being ‘caged’ in regions of space far from excitations, and having to wait for an excitation line to reach its position and allow it to move. As discussed in Ref. [1], the average time it takes a probe to be reached by an excitation line and thus move *for the first time* is the mean persistence time, which is also the  $\alpha$ -relaxation time,  $\tau_\alpha$ , of these models. Further, once the particle has moved, subsequent steps occur when it is hit again by excitation lines, i.e., each time there is a microscopic *exchange* event. The average exchange time,  $\tau_x$ , determines the self-diffusion constant,  $D$ . Since  $\tau_x$  grows much more slowly with decreasing temperature than  $\tau_\alpha$ , the breakdown of the Stokes-Einstein relation follows [1]. This means also that the propagation of the particle is given by a competition between these two fundamental processes: persistence and exchange. Which one dominates at a given temperature will depend on the time and length scales of motion.

To quantify the above observations, we study the histogram of particle displacements, i.e.

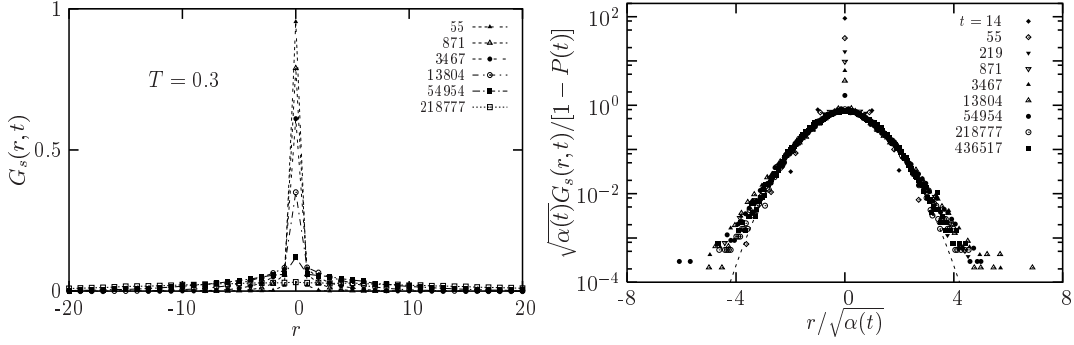


Fig. 2 – Left:  $G_s(r, t)$ , Eq. (1), at fixed temperature and various times has a bimodal form from slow/fast molecules. Right: Diffusive part of  $G_s(r, t)$  rescaled after Eq. (5) shows decreasing deviations from the Gaussian (dashed line) with increasing time.

the self-part of the van Hove function,

$$G_s(r, t) = \left\langle \delta(r - [x(t) - x(0)]) \right\rangle, \quad (1)$$

where brackets indicate an average over trajectories. The above discussion suggests that at times of the order of  $\tau_\alpha$ , some particles are still trapped in their initial position, while others have already escaped and rapidly diffused over a certain distance. The distribution (1) should reflect this bimodal character with a contribution in  $r = 0$  from the ‘slow’, immobile particles, and contributions at non-zero displacements from diffusing, ‘fast’ particles. Numerical results in Fig. 2 (left panel) fully confirm this expectation. Coexistence of fast and slow subpopulations of particles is a major indicator of dynamic heterogeneity [4–7, 15–17].

The behavior of the van Hove function (1) can be anticipated from a simple analysis. Each time the probe particle is allowed to move it makes a random walk step. Therefore, it performs a random walk, but the time lag between steps fluctuates. The time lags are determined by the dynamics of the mobility field of the host liquid. For ease of analysis, we neglect the back reaction of the probe on this field. In this approximation, the probe process is a random walk at random times, or continuous time random walk [18]. The probability for the particle to be at position  $r$  at time  $t$  is then  $G_s(r, t) = \sum_{m=0}^{\infty} \pi_m(t) \phi^{(m)}(r)$ , where  $\pi_m(t)$  is the probability that the probe jumped  $m$  times up to time  $t$ , and  $\phi^{(m)}(r)$  is the probability that a random walker is at site  $r$  after  $m$  steps, having started from the origin.

The first step is a persistence event. If  $p(t)$  is the distribution of persistence times [9], then the probability  $\pi_0(t)$  of not having an event up to time  $t$  is given by  $\pi_0(t) = P(t)$ , where  $P(t) = \int_t^\infty dt' p(t')$  is the persistence function [3, 9]. If we further assume that successive exchange events are uncorrelated, which is a good approximation in the FA model [1], then  $\pi_m(t)$  can be written as a multiple convolution of the exchange time distribution  $\psi(t)$  [19]. The Laplace transform of  $\pi_m(t)$  for  $m > 0$  then reads:  $\hat{\pi}_m(s) = \hat{p}(s) \hat{\psi}^{m-1}(s) [1 - \hat{\psi}(s)]/s$ , where hats indicate Laplace transforms. If we also Fourier transform in space we obtain  $\hat{F}_s(k, s)$ , which is the Laplace transform of the self-intermediate scattering function,  $F_s(k, t)$ , and reads

$$\hat{F}_s(k, s) = \hat{P}(s) + \cos(k) \frac{\hat{p}(s)}{s} \frac{1 - \hat{\psi}(s)}{1 - \cos(k) \hat{\psi}(s)}. \quad (2)$$

This is the Montroll-Weiss equation for the propagator of the probe particle [18]. From Eq. (2)

we immediately obtain a  $k$  and  $T$  dependent timescale:  $\tau(k, T) = \lim_{s \rightarrow 0} \hat{F}_s(k, s)$ . Since the distributions  $p(t)$  and  $\psi(t)$  are both narrow (all moments are finite [3]), their Laplace transforms read, for small  $s$ ,  $\hat{p}(s) \approx 1 - \tau_\alpha s$  and  $\hat{\psi}(s) \approx 1 - \tau_x s$ , which leads to:

$$\tau(k, T) = \tau_\alpha(T) + \frac{\cos(k)}{1 - \cos(k)} \tau_x(T). \quad (3)$$

For small  $k$  this gives  $\tau \approx \tau_\alpha + (k^2 D)^{-1}$ , since  $D = 1/(2\tau_x)$  [1].

The inverse Laplace transform of the factor  $\cos(k)[1 - \hat{\psi}][s - s \cos(k)\hat{\psi}]^{-1}$  in Eq. (2) defines a propagator for diffusing molecules,  $F_{\text{diff}}(k, t)$ . Due to the narrowness of  $\psi$ , it becomes that of normal diffusion in the large  $t$ , small  $k$  limit,  $F_{\text{diff}}(k, t) \approx \exp(-Dk^2 t)$ . Inverse Laplace transforming (2) we obtain  $F_s(k, t) = P(t) + \int_0^t dt' p(t') F_{\text{diff}}(k, t - t')$ . In the regime of strong decoupling this can be further approximated by:

$$F_s(k, t) \approx P(t) + [1 - P(t)] F_{\text{diff}}(k, t). \quad (4)$$

The corresponding van Hove function then reads,

$$G_s(r, t) \approx P(t) \delta(r) + \frac{1 - P(t)}{\sqrt{2\pi\alpha(t)}} \exp\left(-\frac{r^2}{2\alpha(t)}\right), \quad (5)$$

where we have approximated  $G_{\text{diff}}(r, t)$  by a Gaussian for all times. We find that Eq. (5) works well for all times and temperatures, see Fig. 2 (right). Deviations from the Gaussian tend to disappear at long times, as expected. The mean square displacement reads  $\langle r^2 \rangle = \int_{-\infty}^{\infty} dr r^2 G_s(r, t) \simeq [1 - P(t)] \alpha(t)$ , where  $\alpha(t)$  is the mean square displacement obtained by restricting the average to the fast particles. For large times,  $\alpha(t \rightarrow \infty) \approx \langle r^2 \rangle \approx 2Dt$ , while  $\alpha(t \rightarrow 0) = 1$  by construction. Physically, Eq. (5) shows that it is a good approximation to think of molecules as existing in one of two subpopulations of immobile and mobile particles.

Our primary results in this paper all follow from Eq. (5). It is valid only for lengths and times larger than our lattice spacing and unit of time, respectively. Thus the delta-function in Eq. (5) contributes to an experimentally observed  $G_s(r, t)$  only after coarse-graining and would be replaced at smaller length scales by a smoother distribution, typically Gaussian. A two-Gaussian fit to the van Hove function is reported in confocal microscopy experiments performed with colloidal suspensions [15]. If one is predisposed to think of the distribution in terms of a single Gaussian, it will appear as if the distribution has ‘fat tails.’ Such tails have been described as indicators of dynamic heterogeneity [5, 16, 17].

The approximation (5) also provides a simple explanation for the time dependence of the non-Gaussian parameter,  $\alpha_2(t) = \frac{1}{3} \langle r^4 \rangle / \langle r^2 \rangle^2$ . By construction,  $\alpha_2(t) = 1$  for a Gaussian  $G_s(r, t)$ . Instead,  $\alpha_2(t)$  reflects the transition from a Gaussian (fast vibrations at short times) to another Gaussian (Fickian diffusion at long times), the distribution being non-Gaussian at intermediate times when both terms in (5) compete. From Eq. (5) we obtain  $\alpha_2(t) = [1 - P(t)]^{-1}$ , which is monotonically decreasing with time. This expression is valid beyond a coarse graining time, and therefore does not describe the very short-time Gaussian behaviour that would make  $\alpha_2(t)$  non-monotonic. A similar monotonic behaviour is found in molecular dynamics studies of inherent structures dynamics [14]. This expression does, however, explain why  $\alpha_2(t)$  can reach values much larger than unity.

Figure 3 presents our numerical results at various temperatures and wavevectors for the self-intermediate scattering function  $F_s(k, t)$ . At high temperature,  $T = 1.5$ , relaxation is homogeneous and  $F_s(k, t)$  decays exponentially at all wavevectors. The effect of dynamic

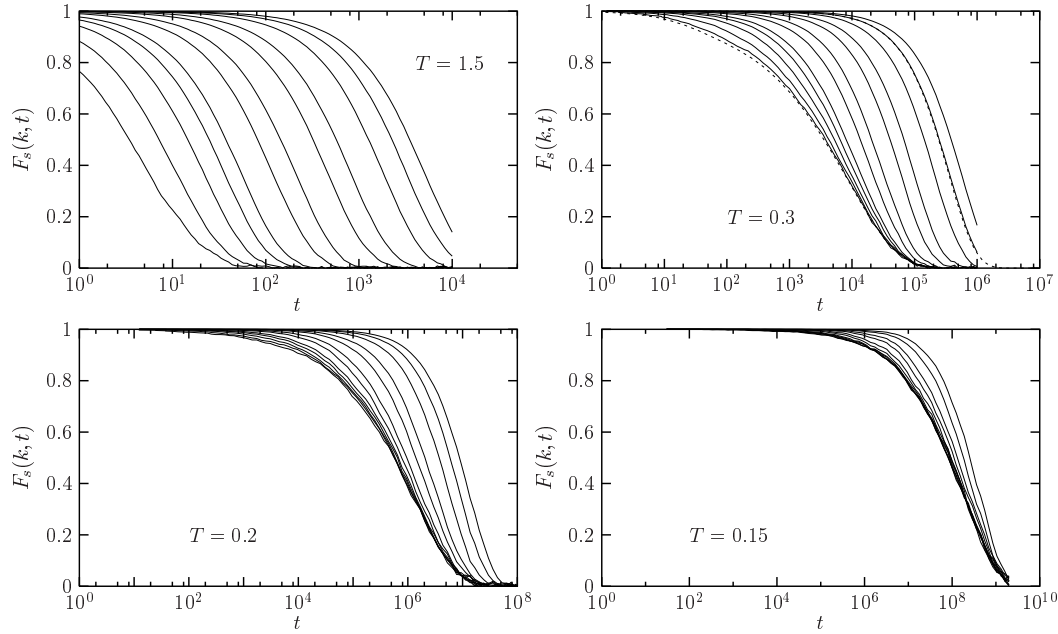


Fig. 3 – Self-intermediate scattering function in the 1D FA model, for different  $T$  and the same range of  $k$ :  $k = 2\pi/n$ , with  $n = 2, 4, 6, 8, 10, 15, 20, 30, 40, 60, 80$ , and  $100$  (from left to right). Dashed lines at  $T = 0.3$  represent the persistence  $P(t)$  and the diffusive behaviour  $\exp[-(2\pi/80)^2 Dt]$ .

heterogeneity becomes fully visible when  $T$  decreases. First, time decays are non-exponential at large wavevector. Second,  $F_s(k, t)$  becomes exponential when  $k$  decreases at constant  $T$ , as suggested by our observations of Fig. 1. Finally, curves for different wavevectors that are distinct at high  $T$  superpose when  $T$  is decreased, and  $F_s(k, t)$  becomes  $k$ -independent.

These observations are rationalized by Eq. (4). For large  $k$ , the last term in (4) is exponentially suppressed, and  $F_s(k, t) \approx P(t)$ , which is  $\exp(-\sqrt{t/\tau_\alpha})$  in the 1D FA model [20]. This behaviour justifies our identification of  $\tau_\alpha$  with the persistence time [1, 9]. At small  $k$  and large times, Eq. (4) becomes  $F_s(k, t) \approx \exp(-k^2 Dt)$ , as confirmed by Fig. 3. At intermediate  $k$ , mixed behaviour between diffusion and persistence is predicted, and observed. These observations naturally imply that stretching is also a  $k$  and  $T$  dependent property, at odds with predictions stemming from mode-coupling theory [22], which indeed poorly describe self-dynamics at intermediate wavevectors [22].

The crossover from persistent to Fickian diffusive dynamics shows up in the behaviour of the relaxation times  $\tau(k, T)$ , as given by Eq. (3). Numerically, we extract the timescales from the scattering functions in the usual way,  $F_s(k, \tau) = e^{-1}$ . Results are presented in Fig. 4. Fickian behaviour,  $\tau \approx k^{-2} D^{-1}$ , is obeyed at all  $k$  at high  $T$ . When  $T$  decreases, diffusive behaviour is restricted to smaller and smaller  $k$ , and is progressively replaced, at larger  $k$ , by the  $k$ -independent form  $\tau \approx \tau_\alpha$ . This leads us to define a temperature dependent characteristic length scale,  $\ell^*(T)$ , which determines the onset of Fickian diffusion. From Eq. (3) we get

$$\ell^* \sim \sqrt{D\tau_\alpha}. \quad (6)$$

It is therefore possible to collapse all timescales on a master curve rescaling times by  $k^{-2} D^{-1}$

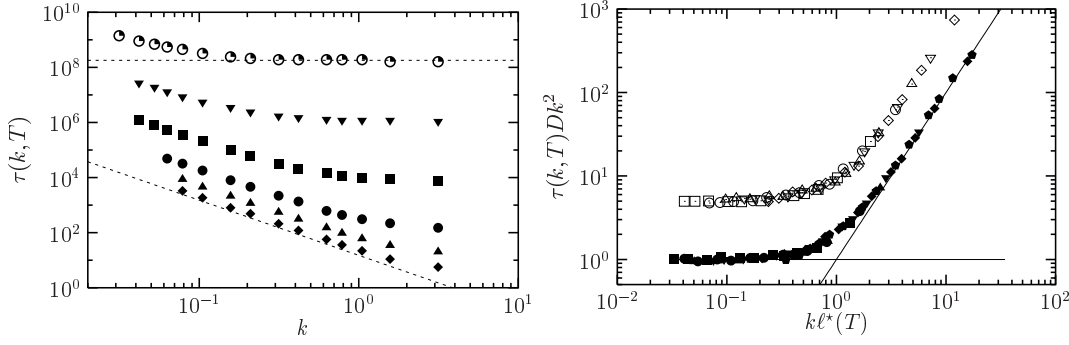


Fig. 4 – Left: Relaxation times in the 1D FA model, as a function of wavevector for different temperatures,  $T = 1.5, 0.8, 0.6, 0.3, 0.2$ , and  $0.15$  (from bottom to top). The straight lines correspond to  $\tau \sim k^{-2}$  and  $\tau \sim \text{const}$ , the limiting behaviours predicted by Eq. (3). Right: timescales rescaled by the diffusive limit  $k^{-2}D^{-1}$  are collapsed using the scaled variable  $k\ell^*$  for both 1D FA (filled symbols) and East (open symbols) models. Data for the East model cover about 10 decades in timescales, with  $T \in [0.31, 0.8]$  and the scaling curve has been shifted by a factor 5, for clarity.

and space by  $\ell^*$ . This is shown in the right panel of Fig. 4, where  $\ell^*$  is estimated from Eq. (6). In Fig. 4, we also show a similar collapse of time scales that we have found when the East model [12] is used in place of the 1D FA model. The East model is the fragile counterpart of the 1D FA model. We see that the scaling behaviour predicted by Eqs. (3, 6) works well also in this case, despite the fact that in the East model successive exchange events are not uncorrelated [1], which was one of the assumptions in the derivation of Eqs. (2)-(5). A behaviour similar to that of Figs. 3 and 4 was recently reported in molecular dynamics simulations of a binary Lennard-Jones mixture [23], and in experiments on supercooled TNB [24].

For both the FA and East models the diffusion constant obeys a fractional Stokes-Einstein law,  $D \sim \tau_\alpha^{-\xi}$ , with  $\xi \leq 1$  [1]. In the case of the FA model,  $\xi_{\text{FA}} = 2/\Delta \approx 2/3, 2/2.3, 2/2.1$  for dimensions  $d = 1, 2, 3$ , respectively,  $\Delta$  being the time exponent  $\tau_\alpha \sim c^{-\Delta}$  [21, 25]. The Stokes-Einstein law,  $\xi = 1$ , is recovered for  $d \geq 4$ , the upper critical dimension of the FA model [21, 25]. For the East model numerical results indicate  $\xi_{\text{East}} \approx 0.7 - 0.8$ , independent of  $d$  up to the highest dimensionality studied,  $d \leq 6$ . Equation (6) can be rewritten,

$$\ell^* \sim \tau_\alpha^{(1-\xi)/2}. \quad (7)$$

Therefore,  $\ell^*$  will diverge when  $T \rightarrow 0$  (or  $c \rightarrow 0$ ) if there is Stokes-Einstein breakdown, i.e., when  $\xi < 1$ . The Fickian crossover length,  $\ell^*$ , measures something related to but distinct from the largest dynamic heterogeneity length,  $\ell(T)$ , which can be measured for example through multi-point dynamic structure factors [6]. For both strong (FA) and fragile (East) systems, this length goes as  $\ell \sim c^{-\nu}$  with a spatial exponent  $\nu$  [3, 25], and therefore always diverges as  $T \rightarrow 0$  in an Arrhenius manner. In general, we have that  $\ell \neq \ell^*$ , and in particular for fragile systems, Eq. (7) shows that  $\ell^*$  will grow faster than  $\ell$ , in a super-Arrhenius way. The reverse is true in strong systems where  $\ell$  should grow faster than  $\ell^*$ . In Ref. [23], the typical length scale  $\ell$  of dynamic heterogeneity was used to rescale wavevectors in the analog of Fig. 4. Present results show instead that  $\ell$  and  $\ell^*$  are different quantities, although they might be hard to distinguish on a restricted temperature window. Finally,  $\ell^*$  was identified in Ref. [26] by dimensional analysis which confuses  $\ell$  and  $\ell^*$ . This particular confusion is avoided in Ref. [27] where the crossover length is also obtained, by assuming a memory function is

analytic for small wave vectors and its Taylor series can be truncated at second order even for wave-vectors that are not small.

The physical basis for the Fickian crossover is that persistence time dominates over exchange time. The former is the time for the first dynamical step, while the latter is the typical time scale of subsequent motion. This mechanism naturally leads to the breakdown of the Stokes-Einstein law [1], non-Gaussian van Hove functions with large tails, and sub-populations of fast and slow particles. The present picture is different from the idea that relaxation and diffusion result from averaging a time and its inverse, respectively, over a single distribution of relaxation times [27, 28]. Our explanation that physically distinct processes (persistence and exchange) compete is consistent with the experimental observation [24] of a strong decoupling in a material with self-similar distributions of relaxation times.

\* \* \*

We are grateful to G. Biroli, Y. Jung, and S. Whitlam for discussions, and to M.D. Ediger and K. Schweizer for discussions about their published and unpublished results. This work was supported by EPSRC Grants No. GR/R83712/01 and GR/S54074/01, E.U. Marie Curie Grant No. HPMF-CT-2002-01927, University of Nottingham Grant No. FEF 3024, the US National Science Foundation, and Oxford Supercomputing Center. Much of this work was carried out in February, 2004, when DC was a Schlumberger Visiting Professor at Oxford.

## REFERENCES

- [1] Y. Jung, J.P. Garrahan, D. Chandler, Phys. Rev. E **69**, 061205 (2004).
- [2] F. Ritort and P. Sollich, Adv. in Phys. **52**, 219 (2003).
- [3] J.P. Garrahan and D. Chandler, Phys. Rev. Lett. **89**, 035704 (2002).
- [4] H. Sillescu, J. Non-Cryst. Solids **243**, 81 (1999).
- [5] M.D. Ediger, Annu. Rev. Phys. Chem. **51**, 99 (2000).
- [6] S.C. Glotzer, J. Non-Cryst. Solids, **274**, 342 (2000).
- [7] R. Richert, J. Phys: Condens. Matter **14**, R703 (2002).
- [8] J.P. Garrahan and D. Chandler, Proc. Natl. Acad. Sci. USA **100**, 9710 (2003).
- [9] L. Berthier and J.P. Garrahan Phys. Rev. E **68**, 041201 (2003).
- [10] L. Berthier and J.P. Garrahan J. Chem. Phys. **119**, 4367 (2003).
- [11] G.H. Fredrickson and H.C. Andersen, Phys. Rev. Lett. **53**, 1244 (1984).
- [12] J. Jäckle and S. Eisinger, Z. Phys. B **84**, 115 (1991).
- [13] T.B. Schröder, S. Sastry, J.C. Dyre, and S.C. Glotzer, J. Chem. Phys. **112**, 9834 (2000).
- [14] C.Y. Liao and S.-H. Chen, Phys. Rev. E **64**, 031202 (2001).
- [15] A. van Blaaderen and P. Wiltzius, Science **270**, 1177 (2000).
- [16] W. Kob *et al.*, Phys. Rev. Lett. **79**, 2827 (1997).
- [17] E.R. Weeks, J.C. Crocker, A.C. Levitt, A. Schofield, and D.A. Weitz, Science **287**, 627 (2000).
- [18] E.W. Montroll and G.H. Weiss, J. Math. Phys. **6**, 167 (1965).
- [19] G.R. Grimmett and D.R. Stirzaker, *Probability and Random Processes* (OUP, Oxford, 1992).
- [20] The functional form of  $P(t)$  is dimensional dependent. See, for example, [21].
- [21] S. Whitlam, L. Berthier, and J.P. Garrahan, cond-mat/0408694.
- [22] W. Götze, J. Phys.: Condens. Matter **11**, A1 (1999).
- [23] L. Berthier, Phys. Rev. E **69**, 020201(R) (2004).
- [24] S.F. Swallen *et al.*, Phys. Rev. Lett. **90**, 015901 (2003); M.D. Ediger *et al.*, unpublished.
- [25] S. Whitlam, L. Berthier, and J.P. Garrahan, Phys. Rev. Lett. **92**, 185705 (2004).
- [26] B.M. Erwin, R.H. Colby, S.Y. Kamath, S.K. Kumar, cond-mat/0409778.
- [27] K.S. Schweizer and E.J. Saltzman, J. Phys. Chem. B, in press (2004).
- [28] G. Tarjus and D. Kivelson, J. Chem. Phys. **103**, 3071 (1995).